



Clinical utility of dynamic-enhanced MRI in salivary gland tumors: retrospective study and literature review

Takenori Ogawa¹ · Ikuho Kojima² · Ryo Ishii¹ · Maya Sakamoto² · Takaki Murata³ · Takahiro Suzuki⁴ · Kengo Kato¹ · Ayako Nakanome¹ · Akira Ohkoshi¹ · Eiichi Ishida¹ · Seiji Kakehata⁵ · Kiyoto Shiga⁶ · Yukio Katori¹

Received: 2 February 2018 / Accepted: 31 March 2018 / Published online: 6 April 2018
© Springer-Verlag GmbH Germany, part of Springer Nature 2018

Abstract

Purpose To improve the diagnoses of the salivary gland tumors, a dynamic-enhanced MRI (dMRI) was investigated.

Methods We conducted a retrospective chart review of 93 cases of salivary gland tumors. The histological diagnoses were obtained from all patients using a surgical specimen and/or an open biopsy specimen. The dMRI as well as fine-needle aspiration cytology (FNAC) and intraoperative frozen section (IFS) were analyzed. This study focused on the time-intensity curve (TIC) after injection, peak time (T_{peak}), washout ratio (WR) as well as the gradient of enhancement and washout profile.

Results The histological diagnoses included pleomorphic adenoma (PMA) in 53 cases, the Warthin tumors (WT) in 14 cases and malignant tumors (MT) in 26 cases. Incorrect diagnosis rate of FNAC and IFS were 5.2 and 8.3%, respectively. The TIC revealed differences among the three types of tumors. T_{peak} as well as WR also revealed significant differences ($p < 0.001$). T_{peak} were lower in order of WT, MT, PMA, respectively. WR of TICs at 30, 45 and 105 s after T_{peak} were higher in order of WT, MT, PMA, respectively ($p < 0.001$). The gradient of increment and washout in the TIC curve was also an important parameter to distinguish the three types of tumors. In MT, the rapid enhancement pattern was found in high or intermediate histological grade tumors, whereas the slow enhancement pattern was exhibited in low grade tumors.

Conclusions Our findings indicate that using T_{peak} and WR, it is possible to distinguish between WT, PMA and MT. Additionally, a rapid enhancement pattern may be a potential marker for these tumors.

Keywords MRI · Dynamic-enhanced MRI · Salivary gland tumor · Diagnosis · Fine-needle aspiration cytology

Introduction

Salivary gland tumors (SGTs) are approximately 3–6% of all head and neck tumors and the annual incidence throughout the world ranges from 0.05 to 2 cases per 100,000

individuals [1]. Pleomorphic adenoma (PMA) and Warthin's tumors (WT) are the most common SGTs among benign tumors [2]. SGTs are classified into 22 different histological types among the malignant tumors (MT) [3].

Surgery is standard treatment for SGTs, however, the surgical procedures of these tumors varies. Complete extirpation is needed not only for MT but also for PMAs due to their malignant transformation potential and recurrence.

Electronic supplementary material The online version of this article (<https://doi.org/10.1007/s00405-018-4965-9>) contains supplementary material, which is available to authorized users.

✉ Takenori Ogawa
ogawa@orl.med.tohoku.ac.jp

¹ Department of Otolaryngology-Head and Neck Surgery, Tohoku University Hospital, 1-1 Seiryomachi, Aoba-ku, Sendai, Miyagi 980-8574, Japan

² Department of Oral Diagnosis, Tohoku University Hospital, 1-1 Seiryomachi, Aoba-ku, Sendai, Miyagi 980-8574, Japan

³ Department of Diagnostic Radiology, Tohoku University Hospital, 1-1 Seiryomachi, Aoba-ku, Sendai, Miyagi 980-8574, Japan

⁴ Department of Otorhinolaryngology, Tohoku Medical and Pharmaceutical University, 4-4-1 Komatsushima, Aobaku, Sendai, Miyagi 981-8558, Japan

⁵ Department of Otolaryngology, Head and Neck Surgery, Yamagata University School of Medicine, Yamagata 990-9585, Japan

⁶ Department of Head and Neck Surgery, Iwate Medical University, Morioka 090-8505, Japan

WTs, on the other hand, have a low incidence of malignant transformation allowing for enucleation or conservative management of the tumor [4, 5]. The surgical treatment strategy for the extirpation of MT and PMA depends on the histological grade and histology of the particular tumor. The facial nerve or its branches are often sacrificed at surgery in high-grade MT, but, can be preserved in cases of low-grade MT as well as in PMAs.

Accurate diagnosis of the type of SGT is important in the creation of a surgical plan. These tumors are usually diagnosed synthetically by the mixture of clinical course, physical findings, imaging and cytological examination. Fine-needle aspiration cytology (FNAC) is useful for diagnosis of these tumors [6, 7], however, false positives and false negatives of MTs can be a problem due to their complicated pathologies [7, 8].

Recently, advanced MRI techniques such as diffusion-weighted MR imaging (DWI), apparent diffusion coefficient (ADC) [9, 10] and dynamic-enhanced MRI (dMRI) [8, 9] have been shown to be effective for the diagnosis of SGTs. A dMRI can estimate the histological diagnosis by time-intensity curve (TIC), however, the efficacy of dMRI for diagnosis of parotid tumors is still unclear [11, 12] and needs further investigation. Here, we analyzed the role of dMRI for pretreatment diagnosis of SGTs retrospectively as well as via a review of recent literature.

Materials and methods

Subjects

We conducted a retrospective chart review of 93 cases of SGTs which underwent a dMRI before treatment at the Tohoku University Hospital. The Institutional Review Board has approved this study [Approved no. 2016-1-754 (Tohoku University Graduate School of Medicine)]. The procedures followed were in accord with the Helsinki Declaration. The histopathological diagnoses were obtained from all patients using a surgical specimen and/or an open biopsy specimen. Histologically, there were 53 PMAs, 14 WTs and 26 MTs (six mucoepidermoid carcinomas, three carcinomas ex

two metastatic carcinomas). Neither recurrent nor secondary tumors were observed in the study group. High, intermediate and low-grade MTs were diagnosed by previous criteria [1, 3].

MRI technique

MR examinations were performed using a 1.5 T MR imager (Signa Horizon LX CVi; GE Medical Systems, Milwaukee, WI, USA) with either quadrature head neck vascular or surface coil. Postcontrast transverse T1-weighted images (TR/TE/number of signal acquisitions 460–646 ms/12–15 ms/1) were obtained using a spin-echo sequence with a scanning delay time of 133–189 s after dynamic study, field of view (FOV) 210 mm, slice thickness 5 mm, slice gap 1 mm, and acquisition matrix size 320 × 256. For dynamic contrast-enhanced studies, transverse T1-weighted images (TR/TE/number of signal acquisition 135 msec/8 msec/1) were obtained using a turbo spin-echo sequence, FOV 280 mm, slice thickness 5 mm, slice gap 1 mm, and acquisition matrix size of 256 × 128. Gadolinium (Magnevist; Bayer Health Care, Osaka, Japan) was injected intravenously at a dose of 0.2 mL/kg body weight. In each patient, eight scans were obtained at an interval of 15 s. MR images were sequentially obtained 0, 15, 30, 45, 60, 75, 90, and 105 s after contrast medium injection initiation. Gd-DTPA was administered at the beginning of the first scan and is designated as time 0. One (or Two) author(s) (M. S. and T. M.) manually drew regions of interest (ROIs) to avoid the vessels and cystic parts of the tumors, in reference to contrast-enhanced transverse T1-weighted images. We plotted the signal intensity within the ROI against time, and TICs were constructed by modified increment ratios where $(IR) = \frac{((\text{signal intensity}) - (\text{pre-enhancement signal intensity})) \times 100}{\text{pre-enhancement signal intensity}}$ as has been reported previously [13].

MR factor analysis

MR images were interpreted retrospectively by three readers T. M., M. S. and I. K. before histological diagnoses. Based on the TICs, the MR factor analysis such as the time to peak enhancement (T_{peak}) and the washout ratio (WR) (%):

$$WR = \frac{((\text{peak signal intensity}) - (\text{intensity 105 s after contrast injection})) \times 100}{(\text{peak signal intensity}) - (\text{signal intensity of pre-enhancement})}$$

pleomorphic adenoma, two squamous cell carcinomas, four salivary duct carcinomas, two malignant lymphomas, two adenocarcinomas, one basal celladenocarcinoma, one epithelial–myoepithelial carcinoma, one true carcinosarcoma, one acinic cell carcinoma, one myoepithelial carcinoma, and

were analyzed.

The gradient of IR and WR in TIC curve was also analyzed as a role of parameter to divide three types of tumors at 15 s after injection or peak time. The rapid enhancement was defined when

$$IR_{15s} = \frac{((\text{signal intensity } 15 \text{ s}) - (\text{pre-enhancement signal intensity})) \times 100}{\text{pre-enhancement signal intensity}}$$

was more than 100. WR_{15s} was calculated by the following formula;

$$WR_{15s} (\%) = \frac{((\text{peak signal intensity}) - (\text{intensity } 15 \text{ s after Tpeak})) \times 100}{(\text{peak signal intensity}) - (\text{signal intensity of pre-enhancement})}$$

WR_{15s} was also divided as rapid (more than +10%), plateau (-10 to +10%) and negative (peak time was 105 s).

These dMRI factors as well as FNAC and IFS were compared among PMA, WT, low- and high-grade MT.

Statistical analysis

We used the Kruskal–Wallis rank sum test to compare continuous variates among three groups, adding the Holm test as post hoc analysis. To quantify the accuracy of diagnosis, we drew the receiver operator characteristic (ROC) curve, in which we defined cut-off values by Youden index. We also calculated positive predictive value (PPV), negative predictive value (NPV), and accuracy with the above cut-off values. A *p* value < 0.05 was considered significant, and all tests

were two tailed. All statistical analyses were performed with R for Windows (version 2.0-3) and EZR (version 1.36) [14].

Result

Patient characteristics

Patient characteristics were shown in Table 1. The cases included 43 males and 50 females, aged from 16 to 89 years (median age 63 years). The histological diagnoses included PMA in 53 cases, WT in 14 cases and MT in 26 cases. Most PMA and WT patients were in the 0s, while MT patients were in their 70 s.

Accuracy of FNAC and IFS

FNAC was performed in 77 cases (Table 2). Among them, insufficient materials were found in seven cases. One case of PMA was diagnosed as adenoid cystic carcinoma and three

Table 1 Patients’ profiles

Histology	Number of patients	Gender M/F	Age						
			~29	30–39	40–49	50–59	60–69	70–79	80 ~
PMA	53	16/37	5	6	6	13	15	7	1
Malignancy	26	16/10	3			2	4	13	4
WT	14	11/3		1	1	4	5	3	
Total	93	43/50	8	7	7	19	24	23	5

Table 2 The results of FNAC and IFS

Histology	FNAC/total patients	FNAC class						IFS/total patients	IFS diagnosis	
		Insufficient	I	II	III	IV	V		Correct	Incorrect
PMA	46/53	6	3	31	5	0	1 ^a	27/53	27	0
Malignancy	19/26	1	1 ^b	2 ^b	6	2	7	18/26	14	4 ^c
WT	12/14	0	2	10	0	0	0	3/14	3	0
Total	77/93							48/93		

FNAC fine needle aspiration cytology, IFS intraoperative frozen section

^aThis case was diagnosed as adenoid cystic carcinoma ex PMA by FNAC, however, final diagnosis was PMA without malignant transformation

^bThree cases consist of acinic cell carcinoma, low-grade mucoepidermoid carcinoma and diffuse large B cell lymphoma

^cFour cases consisting of low-grade mucoepidermoid carcinoma, low-grade basal cell adenocarcinoma, epithelial–myoepithelial carcinoma and true carcinosarcoma were diagnosed as benign tumors by IFS

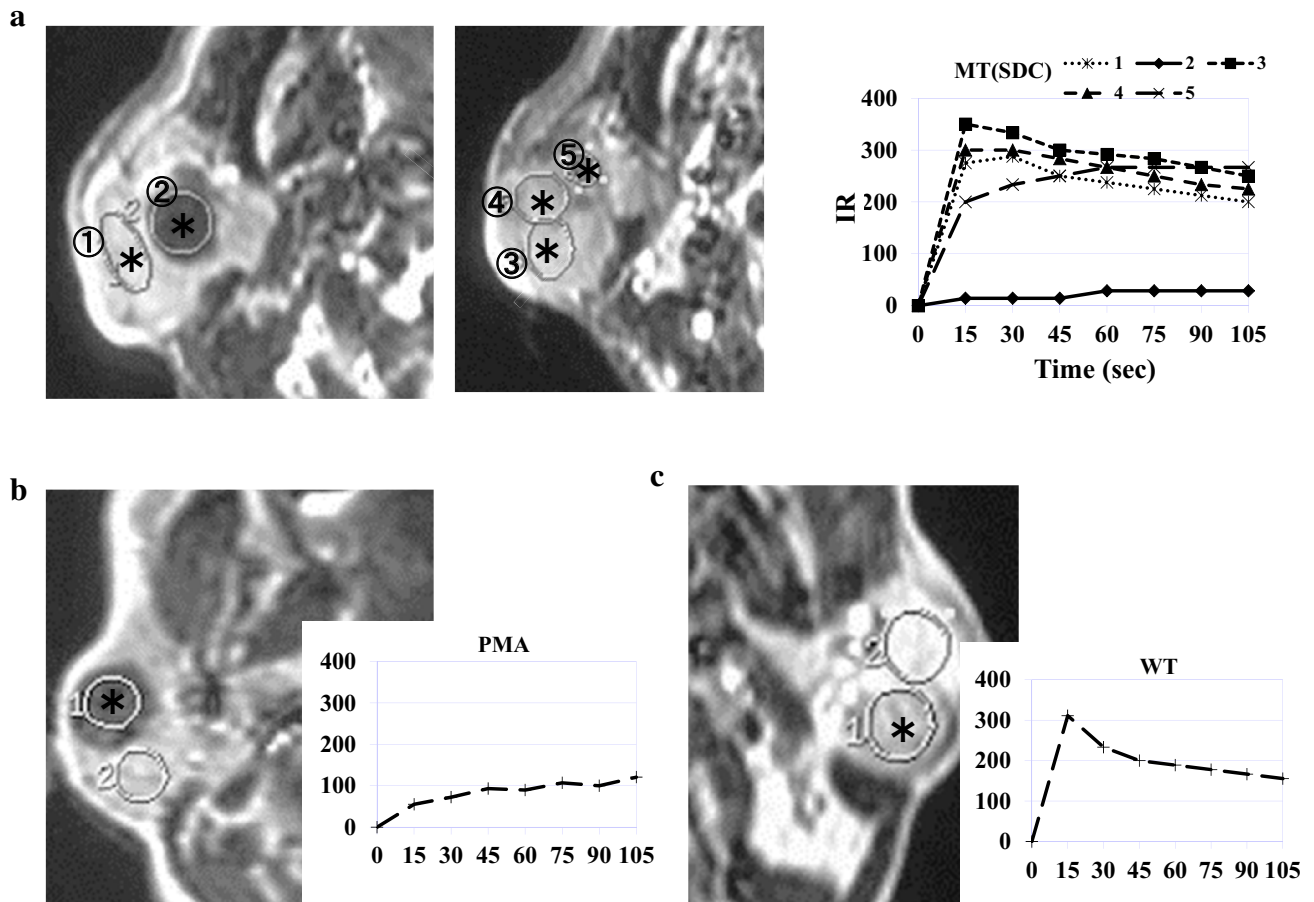


Fig. 1 MRI images and TICs of SGTs. **a** Salivary duct carcinoma (SDC), asterisks indicate tumor. Four ROIs (#1, 3, 4 and 5) in TIC indicated the typical MT patterns while only one ROI (#2) of the

cystic component indicated no enhancement. **b** PMA, **c** WT. Asterisks indicate tumor. ROIs of normal gland (#2) were not shown

cases of MT (acinic cell carcinoma, low-grade mucoepidermoid carcinoma and diffuse large B cell lymphoma) were diagnosed as benign by FNAC. IFS was performed in 48 cases (Table 2). Among them, four cases of MT (low-grade mucoepidermoid carcinoma, low grade basal cell adenocarcinoma, epithelial–myoepithelial carcinoma and true carcinosarcoma) were diagnosed as benign tumors. As such, prior to any histological examination, the incorrect diagnosis rate of FNAC and IFS, with respect to malignancy, was 5.2 and 8.3%, respectively.

Dynamic-enhanced MRI analysis

Dynamic-enhanced MRI was performed in all 93 cases. The representative cases with MT, PMA and WT are shown in Fig. 1. TIC patterns were different between solid and cystic parts of the same salivary duct carcinoma (Fig. 1a), thus, for diagnosis, cystic and vessel parts were excluded by drawing ROIs as indicated on the contrast-enhanced transverse T1-weighted images. The raw TICs of all cases are shown in

Fig. 2. The TICs presented characteristic findings according to histologic type. IR at 15, 45, 75 and 105 s revealed differences between each histologic type as well. Tpeak was lower in order of PMA (median 105 s, mean 96.2 ± 14.5 s), MT (median 45 s, mean 51.4 ± 30.5 s) and WT (median 21.4 s, mean 15 ± 7.7 s), with statistical significance ($p < 0.001$) (Fig. 3a and supplementary Fig. 1). ROC curve of each histologic type by peak time was also shown in Fig. 3. Area under the curve (AUC) of MT, PMA and WT were 0.739, 0.925 and 0.939, respectively. Cut-off value by peak time was calculated with 75 s for MT (sensitivity 80.8, specificity 67.2%, PPV 48.8%, NPV 90.0%, accuracy 71.0%), 60 s for PMA (sensitivity 100%, specificity 72.5%, PPV 82.8%, NPV 100%, accuracy 88.8%) and 30 s for WT (sensitivity 100%, specificity 86.1%, PPV 56.0%, NPV 100%, accuracy 88.2%), respectively. WR at 30, 45 and 105 s after peak were ranked from high to low in the order WT, MT and PMA with a statistically significant difference ($p < 0.001$) (Fig. 4 and supplementary Fig. 2). The ROC curve of each histologic type by washout ratio at 45 s after peak time is shown in

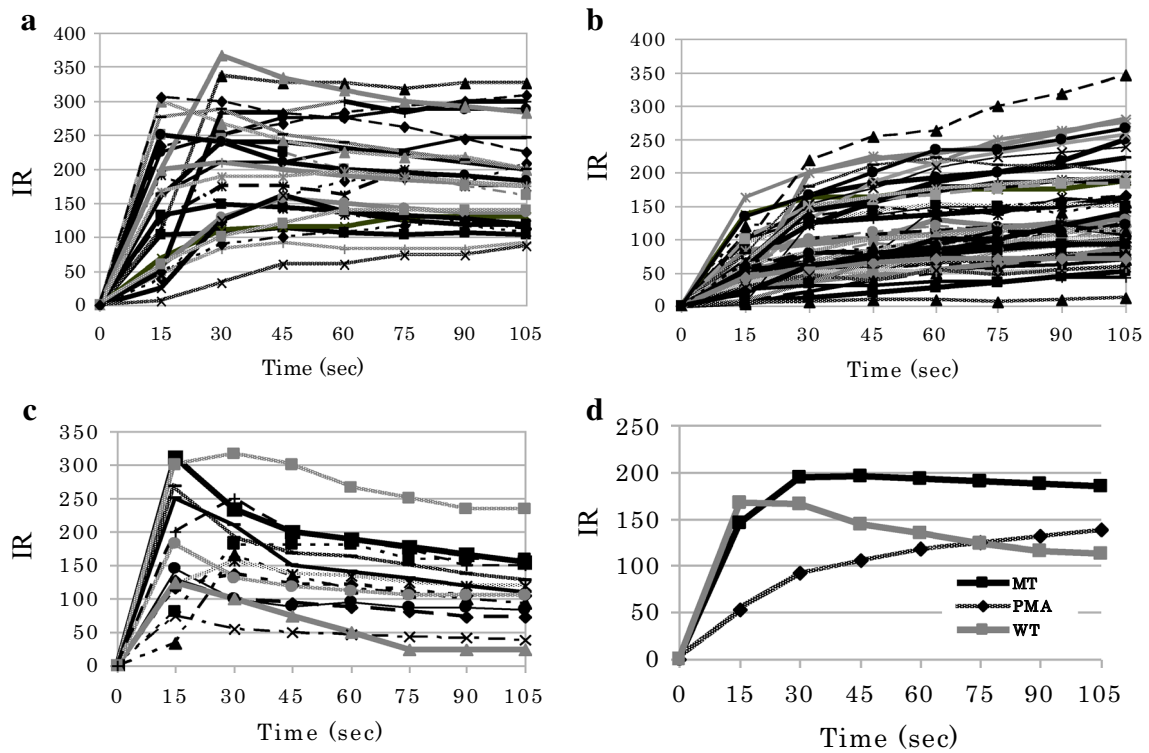


Fig. 2 TICs of all parotid tumors. a MT, b PMA, c WT, d average of each SGT

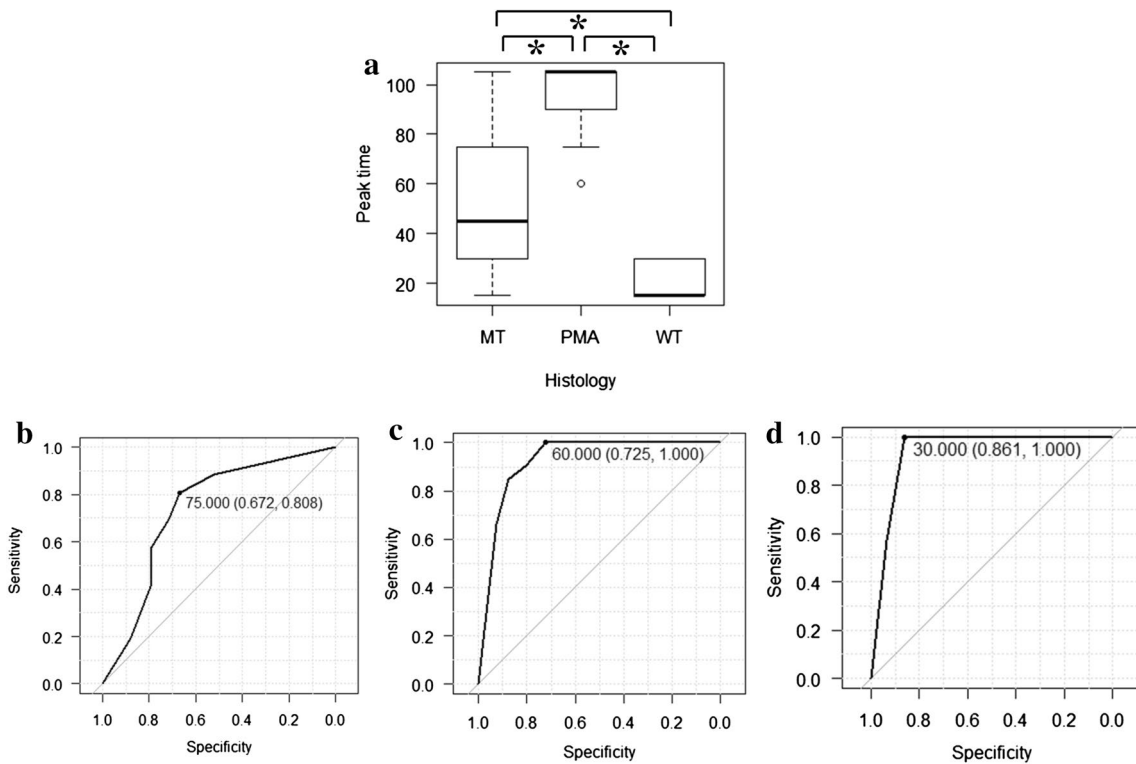


Fig. 3 Tpeak of TICs. a The box and whisker plot, b ROC curve of peak time in parotid tumors (left: MT, middle: PMA, right: WT). * $p < 0.001$

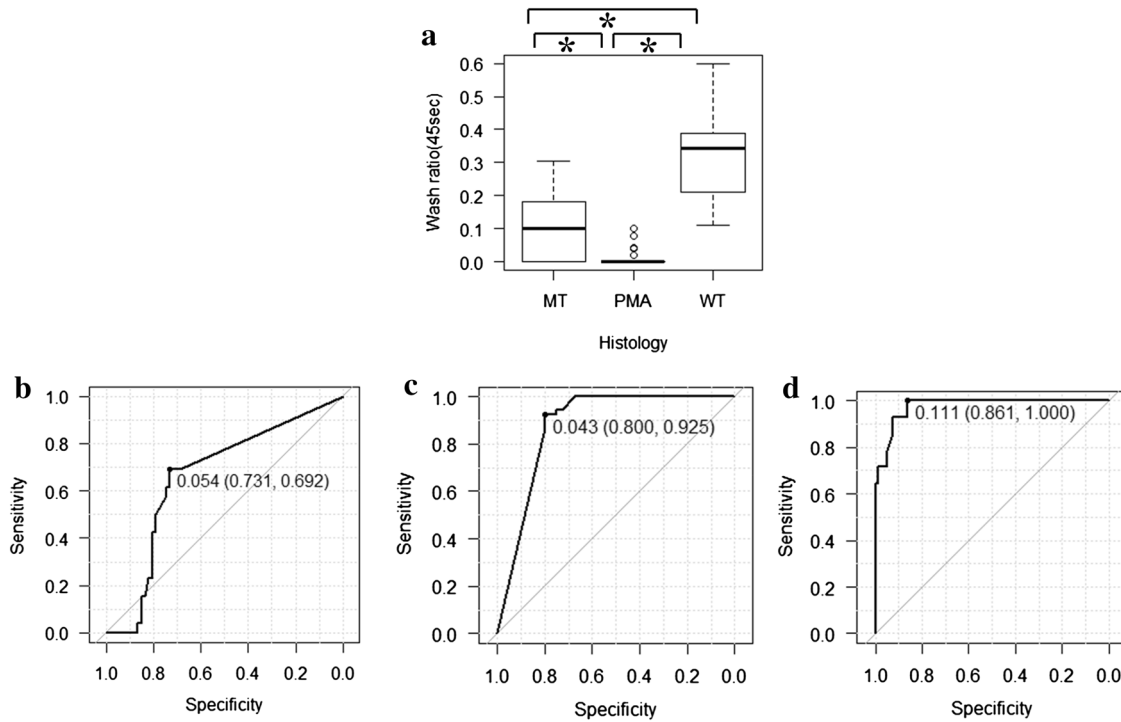


Fig. 4 ROC curve of WR at 45 s after Tpeak. a MT, b PMA, c WT

Table 3 Representative patterns of the enhancement/washout as predictors of tumor type

Tumor type	dMRI enhancement/washout pattern
WT	Rapid enhancement ► rapid washout
PMA	Slow enhancement ► plateau or negative washout
MT	Rapid or slow enhancement ► plateau washout

Table 4 The results of a gradient of enhancement among histological grade of MT

Histological grade	Enhancement	
	Rapid	Slow
Low	2	4
Intermediate	3	1
High	12	4

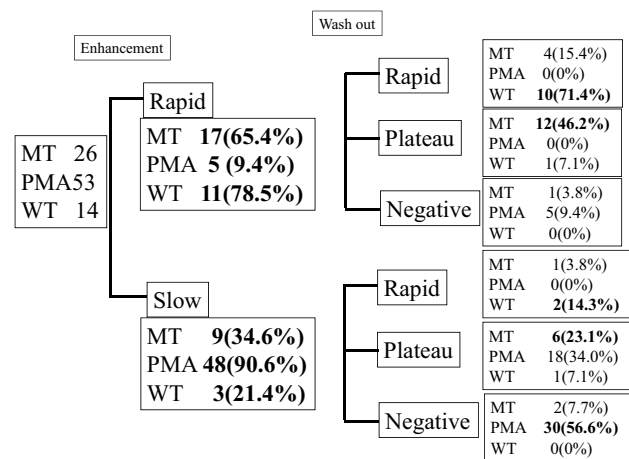


Fig. 5 Algorithm by a gradient of enhancement and washout

Fig. 4. The 45 s mark was chosen because the washout ratio after Tpeak exhibited the lowest p value ($p = 1.03 \times 10^{-13}$). The AUC of MT, PMA and WT were 0.661, 0.88 and 0.976, respectively. Cut-off value by WR was calculated with 5.4% for MT (sensitivity 69.2%, specificity 73.1%, PPV 48.6%, NPV 85.7%, accuracy 71.0%), 4.3% for PMA (sensitivity 92.5%, specificity 80%, PPV 85.7%, NPV 86.5%, accuracy 86.0%) and 11.1% for WT (sensitivity 100%, specificity 86.1%, PPV 56.0%, NPV 100%, accuracy 88.2%).

We observed that the TIC divided into six patterns of enhancement and washout. Of the six patterns observed, three patterns emerged as predictors of tumor type, shown in Table 3. 10 of the 14 WTs (71.4%) showed rapid enhancement—rapid washout. 48 of 53 PMAs (90.6%) showed the slow enhancement—plateau or negative washout pattern (Fig. 5). For MTs, rapid or slow enhancement—plateau washout pattern in 18 of the 26 cases (69.3%). Table 4 showed the enhancement pattern among histological grade

Table 5 Literature review of the efficacy of dMRI for diagnosis of SMG

References	Year	Tesla	Histology	n	Parameter	Sensitivity	Specificity	PPV	NPV	Accuracy
Wang et al. [15]	2001	1.5	Total	97	MT: ADC < 1.22 × 10 ⁻³ mm ² /s	84	91			86
Yabuuchi et al. [16]	2003	0.5	MT	11	Tpeak ≤ 120, WR < 30%	90.9	90.5	83.3	95	90.6
			PMA	12	Tpeak > 120	75	100	100	87	90.6
Eida et al. [17]	2007	1.5	WT	9	Tpeak ≤ 120, WR ≥ 30%	88.9	95.7	88.9	95.7	93.8
			Total	31	BT: ADC ≥ 1.8 × 10 ⁻³ mm ² /s	89	100	100	96	97
Eida et al. [18]	2010	1.5	MT	18	Tpeak ≤ 120, WR < 30%	44.4	100	100	83.1	85.1
			PMA	28	Tpeak > 120	100	82.1	80	100	90
Yabuuchi et al. [9]	2008	1.5	WT	21	Tpeak ≤ 120, WR ≥ 30%	100	93.5	87.5	100	95.5
			MT	14	Tpeak ≤ 120, WR < 30%	71.4	85.3	66.7	87.9	81.3
			PMA	20	Tpeak > 120	75	96.4	93.8	84.4	87.5
			WT	14	Tpeak ≤ 120, WR ≥ 30%	100	91.2	82.4	100	93.8
The above were summarized by Assili et al. [19]										
Histomi et al. [20]	2007	1.5	MT	12	60 < Tpeak < 210, 10% < WR ₃₀₀ < 30%	50	97.1	85.7	85	85.1
			PMA	20	Tpeak > 210, WR ₃₀₀ < 10%	70	100	100	81.8	87.2
			WT	15	Tpeak < 60, WR ₃₀₀ > 40%	93.3	100	100	97	97.9
Aghaghazvini et al. [21]	2015	3.0	MT	10	Tpeak < 43 s and WR ₁₈₀ = 4.6–22.0%	60	97	85.7	88.9	88.4
			PMA	27	Tpeak > 43 s and WR ₁₈₀ < 4.6%	96.3	87.5	92.9	93.3	93
			WT	6	Tpeak < 43 s and WR ₁₈₀ > 22.0%	100	94.6	75	100	95.3
Lam et al. [22]	2015	1.5	MT	24	MT: Tpeak < 150 s, WR < 30%	79.2	94.6	82.6	93.3	90.8
			BT	74						
Mikaszewski et al. [12]	2017	1.5	MT	19	Tpeak < 120 s and WR > 30%	89.5	100	100	97.1	97.7
			PMA	29	Tpeak > 120 s and WR < 10%					
			WT	38	Tpeak < 120 s and WR > 30%					
Tao et al. [23]	2017	1.5	Other BT	14						
			MT	47	MT: ADC < 1.12 × 10 ⁻³ and plateau (TIC)	85.1	94.1	87	93.1	91.2
This study		1.5	BT	101						
			MT	26	Tpeak < 105, WR < 30%	73.1	94	82.6	90	88.2
			PMA	53	IR _{15s} > 100 and WR _{15s} > 10%	46.1	98.5	92.3	82.5	83.9
			WT	14	Tpeak ≥ 105 s and WR < 10%	66	92.5	92.1	67.3	77.4
					IR _{15s} < 100	90.6	70	80	84.8	81.7
					Tpeak < 105, WR ≥ 30%	71.4	94.9	71.4	94.9	91.4
					IR _{15s} > 100 and WR _{15s} > 10%	71.4	94.9	71.4	94.9	91.4

PPV positive predicting value, NPV negative predicting value

of MTs. Rapid enhancement showed in 2 cases (33.3%) of low grade MTs, 3 cases (75%) of intermediate and 12 cases (75%) of high-grade MTs. Slow enhancement observed in four cases (66.7%) of low-grade MTs, one case (25%) of intermediate and three cases (25%) of high-grade MTs ($p=0.252$).

Literature review

The sensitivity, specificity, PPV, NPV and accuracy of dMRI from the previous literature are summarized in Table 5. Accuracy was higher in order of WT (91.4–97.9%), MT (81.3–97.7%) and PMA (77.4–93%).

Discussion

Pretreatment diagnosis of SGTs can be difficult. FNAC is considered the gold standard for the diagnosis of SGTs with an overall accuracy of 95%, however, false negatives of MTs [7] and false positive of PMA [7] and WT [8] sometimes occur. In this study, in the absence of any histological analysis, the incorrect diagnosis rate of FNAC was 5.2% where one case of PMA without malignant transformation was diagnosed as adenoid cystic carcinoma as diagnosed by FNAC and three cases consisted of acinic cell carcinoma, low-grade mucoepidermoid carcinoma and diffuse large B cell lymphoma diagnosed as class I or II (benign tumors) by FNAC.

It has been previously reported that, using conventional MRI techniques, it is possible to distinguish malignant from benign tumors. For example, tumors with well-defined borders tend to be benign as is the case for PMAs and WTs [24]. In addition, high signal intensity on T2-weighted images are typical of PMAs [25], whereas low signal intensity is a sign of malignancy [25]. However, because low T2 signal intensity is also present with WTs, determination of tumor type can remain uncertain [26]. Using dMRI results, Hisatomi et al. have reported characteristic TIC patterns of SGTs [27, 28]. Their research indicates that rapid increase, low Tpeak, and high WR are recognized as a characteristic pattern of WTs and high Tpeak with low WR as a characteristic pattern of PMAs. Asseli et al. also examined the efficacy of dMRI for pretreatment diagnoses from the previous literature [19] and despite the use of several different cut-off values, Tpeak and WR were shown to also be useful parameters to distinguish various SGTs.

In this study, using the TIC of dMRI, a histologically specific pattern emerged. Of the total six enhancement/washout patterns observed, three patterns were determined to be predictors of SGT type. In addition, by examining the AUC of Tpeak and the WR, unique cut-off values for MT and PMA were observed. Unfortunately, these cut-off values

were too close to each other to be useful. Previous data as well as this study have shown that WTs are likely the best candidate for the use of dMRI since it has the highest accuracy among three histological types. In fact, the WT pattern was clearly highlighted with a $T_{peak} < 105$ s and $WR \geq 30\%$ in this study giving it an accuracy of 91.4%. To distinguish MT from PMA, this study indicated that a rapid enhancement pattern along with Tpeak and WR values could be potential markers. It should be noted that the enhancement pattern depends on the histological grade of MTs, with slow enhancement in low-grade MTs and rapid enhancement in intermediate and high-grade MTs. These results seem to be helpful in that high-grade MT can be distinguished from low-grade MT/PMA from the viewpoint of facial nerve preservation and WT can be distinguished from the other SGT for observational strategies. It has been reported that Tpeak correlates closely with tumor vascularity and the washout ratio accurately reflected the cellularity-stromal grade [16], as such, rapid enhancement as well as short Tpeak may be influenced by high tumor vascularity.

According to the literature review, accuracy was higher in the order of WT (91.4–97.9%), MT (81.3–97.7%) and PMA (77.4–93%). Our study also followed this same order of accuracy. Furthermore, since it is reported that addition of the ADC value to the Tpeak leads to improved differentiation of MT from PMA [9, 23], especially with new diagnostic algorithms [12] and a multiparametric approach based on a combination of parameters [29], ADC and dMRI could become a future screening method.

Since this was a limited retrospective study, a prospective study is, therefore, considered to be necessary to further validate our hypothesis and that more patients should be enrolled to obtain a stronger statistical significance for these results.

Conclusion

Our results indicate that dMRI can be a useful quantitative preoperative tool in the treatment of salivary gland tumors, especially WTs. To distinguish MT from PMA, this study indicates that a rapid enhancement pattern as well as Tpeak and WR could be potential markers for these tumors.

Acknowledgements We are grateful to Miles Kuperus for editorial work in the preparation of this manuscript.

Compliance with ethical standards

Conflict of interest We declare no conflict of interest.

Ethical approval All procedures performed in studies involving human participants were in accordance with the ethical standards of the insti-

tutional and/or national research committee and with the 1964 Helsinki Declaration and its later amendments or comparable ethical standards.

Informed consent Informed consent was obtained from all individual participants included in the study. The Institutional Review Board has approved this study [Approved no. 2016-1-754 (Tohoku University Graduate School of Medicine)].

References

- Guzzo M, Locati LD, Prott FJ, Gatta G, McGurk M, Licitra L (2010) Major and minor salivary gland tumors. *Crit Rev Oncol Hematol* 74:134–138
- Lin CC, Tsai MH, Huang CC, Hua CH, Tseng HC, Huang ST (2008) Parotid tumors: a 10-year experience. *Am J Otolaryngol* 29:94–100
- Brandwein-Gensier M, Bell D, Inagaki H et al (2017) Tumours of salivary glands. In: El-Naggar AK, Chan JK, Grandis JR, Takata T, Slootweg PJ (eds) WHO classification of head and neck tumours, 4th edn. IARC, Lyon, pp 160–202
- Reddy VM, Thangarajah T, Castellanos-Arango F, Panarese A (2008) Conservative management of Warthin tumour. *J Otolaryngol Head Neck Surg* 37:744–749
- Teymoortash A, Werner JA (2005) Tissue that has lost its track: Warthin's tumour. *Virchows Arch* 446:585–588
- Veder LL, Kerrebijn JD, Smedts FM, den Bakker MA (2010) Diagnostic accuracy of fine-needle aspiration cytology in Warthin tumors. *Head Neck* 32:1635–1640
- Gudmundsson JK, Ajan A, Abtahi J (2016) The accuracy of fine-needle aspiration cytology for diagnosis of parotid gland masses: a clinicopathological study of 114 patients. *J Appl Oral Sci* 24:561–567
- Ogawa T, Suzuki T, Sakamoto M et al (2012) Correct diagnosis of Warthin tumor in the parotid gland with dynamic MRI. *Tohoku J Exp Med* 227:53–57
- Yabuuchi H, Fukuya T, Tajima T, Hachitanda Y, Tomita K, Koga M (2008) Parotid gland tumors: can addition of diffusion-weighted mr imaging to dynamic contrast enhanced MR imaging improve diagnostic accuracy in characterization? *Radiology* 249:909–916
- Yuan Y, Tang W, Tao X (2016) Parotid gland lesions: separate and combined diagnostic value of conventional MRI, diffusion-weighted imaging and dynamic contrast-enhanced MRI. *Br J Radiol* 89(1060):20150912
- Stefanovic X, Al Tabaa Y, Gascou G et al (2017) Magnetic resonance imaging of parotid gland tumors: dynamic contrast-enhanced sequence evaluation. *J Comput Assist Tomogr* 41:541–546
- Mikaszewski B, Markiet K, Smugała A, Stodulski D, Szurowska E, Stankiewicz C (2017) Diffusion- and perfusion-weighted magnetic resonance imaging—an alternative to fine needle biopsy or only an adjunct test in preoperative differential diagnostics of malignant and benign parotid tumors? *J Oral Maxillofac Surg* 75:2248–2253
- Eida S, Ohki M, Sumi M, Yamada T, Nakamura T (2008) MR factor analysis: improved technology for the assessment of 2D dynamic structures of benign and malignant salivary gland tumors. *J Magn Reson Imaging* 27:1256–1262
- Kanda Y (2013) Investigation of the freely available easy-to-use software 'EZR' for medical statistics. *Bone Marrow Transpl* 48:452–458
- Wang J, Takashima S, Takayama F et al (2001) Head and neck lesions: characterization with diffusion-weighted echoplanar MR imaging. *Radiology* 220:621–630
- Yabuuchi H, Fukuya T, Tajima T, Hachitanda Y, Tomita K, Koga M (2003) Salivary gland tumors: diagnostic value of gadolinium-enhanced dynamic MR imaging with histopathologic correlation. *Radiology* 226:345–354
- Eida S, Sumi M, Sakihama N, Takahashi H, Nakamura T (2007) Apparent diffusion coefficient mapping of salivary gland tumors: prediction of the benignancy and malignancy. *Am J Neuroradiol* 28:116–121
- Eida S, Sumi M, Nakamura T (2010) Multiparametric magnetic resonance imaging for the differentiation between benign and malignant salivary gland tumors. *J Magn Reson Imaging* 31:673–679
- Assili S, Fathi KA, Aghaghazvini L, Saligheh RHR, Pirayesh IJ (2015) Dynamic contrast magnetic resonance imaging (DCE-MRI) and diffusion weighted MR imaging (DWI) for differentiation between benign and malignant salivary gland tumors. *J Biomed Phys Eng* 5:157–168
- Hisatomi M, Asaumi J, Yanagi Y et al (2007) Diagnostic value of dynamic contrast-enhanced MRI in the salivary gland tumors. *Oral Oncol* 43:940–947
- Aghaghazvini L, Salahshour F, Yazdani N et al (2015) Dynamic contrast-enhanced MRI for differentiation of major salivary glands neoplasms, a 3-T MRI study. *Dentomaxillofac Radiol* 44:20140166
- Lam PD, Kuribayashi A, Imaizumi A et al (2015) Differentiating benign and malignant salivary gland tumours: diagnostic criteria and the accuracy of dynamic contrast-enhanced MRI with high temporal resolution. *Br J Radiol* 88(1049):20140685
- Tao X, Yang G, Wang P et al (2017) The value of combining conventional, diffusion-weighted and dynamic contrast-enhanced MR imaging for the diagnosis of parotid gland tumours. *Dentomaxillofac Radiol* 46:20160434
- Thoeny HC (2007) Imaging of salivary gland tumours. *Cancer Imaging* 7:52–62
- Christe A, Waldherr C, Hallett R, Zbaeren P, Thoeny H (2011) MR imaging of parotid tumors: typical lesion characteristics in MR imaging improve discrimination between benign and malignant disease. *Am J Neuroradiol* 32:1202–1207
- Okahara M, Kiyosue H, Hori Y, Matsumoto A, Mori H, Yokoyama S (2003) Parotid tumors: MR imaging with pathological correlation. *Eur Radiol* 13(Suppl 4):L25–L33
- Hisatomi M, Asaumi J, Konouchi H, Yanagi Y, Matsuzaki H, Kishi K (2002) Assessment of dynamic MRI of Warthin's tumors arising as multiple lesions in the parotid glands. *Oral Oncol* 38:369–372
- Hisatomi M, Asaumi J, Yanagi Y et al (2003) Assessment of pleomorphic adenomas using MRI and dynamic contrast enhanced MRI. *Oral Oncol* 39:574–579
- Patella F, Franceschelli G, Petrillo M et al (2018) A multiparametric analysis combining DCE-MRI- and IVIM -derived parameters to improve differentiation of parotid tumors: a pilot study. *Future Oncol*. <https://doi.org/10.2217/fo-2017-0655>